





















observed fiber dispersion (Fig. 1), yielding a value of  $0.037 \text{ (W}\cdot\text{m)}^{-1}$  at the laser wavelength of 1041 nm. The peak incident power  $P_0$  can be calculated from  $P_0 = P/(2T_0R)$ , where  $P$  is the fiber output power (0.361 W),  $R$  is the known repetition rate of the laser pulses (76 MHz), and  $T_0$  is 130 fs. This method results in a  $L_{0.361}$  value of 1.48 mm, which is close to the value shown in Table 2. The discrepancy may be attributed to the systematic readout error of the power meter and/or the uncertainty in calculating  $\gamma$ . The merit of writing the scalar GNLSE in the form of Eq. (1) lies in the combination of  $\gamma$  and  $P_0$  into one single parameter  $L_{\text{NL}}$ , so that the scalar GNLSE can be calculated with a minimum number of parameters (Table 2).

#### 4.4 Aspects of rigorous quantification

The effect of  $L_{\text{NL}}$  (or equivalently, fiber input power) on the spectrum of the continuum pulses can be appreciated in Fig. 4(a)–4(d). Also, the effect of dispersion can be appreciated by setting all dispersion coefficients  $\beta_k$  in Eq. (1) to zero, and then performing the same simulation [Fig. 4(e)]. Finally, the effect of the initial pulse chirp of  $8500 \text{ fs}^2$  can be appreciated by removing this chirp and then performing the same simulation [Fig. 4(f)]. These exercises demonstrate the sensitivity of the continuum spectrum to the parameters of  $C$ ,  $\Lambda$ ,  $d/\Lambda$ , and  $L_{0.361}$ . Extensive simulations reveal that each value of  $C$ ,  $\Lambda$ ,  $d/\Lambda$ , and  $L_{0.361}$  must not deviate by 10% from that given in Table 2 to ensure a high-quality agreement between the simulated and observed spectra if the values of the other parameters in Table 2 are fixed. In other words, the values of these four parameters in Table 2 do not need to be known *a priori*. They can be independently determined with a relative error of less than 10% by simply matching the simulated and observed spectra.

The above sensitivity suggests that the theoretical reproduction of the observed spectral fringes require the scalar GNLSE, not one of its simplified forms. To verify this, we replace the terms on the right hand side of Eq. (1) with a single term that represents the self phase modulation (SPM) [28], and perform the same simulation using the same values of  $C$ ,  $\Lambda$ ,  $d/\Lambda$ , and  $L_{0.361}$  [Fig. 4(g)]. Although this simulation largely reproduces the general trend of the spectral fringes, the simulated spectrum deviates substantially from the observed spectrum. Somewhat surprisingly, the observed spectra can be used to discriminate the incident soliton (sech) pulses against Gaussian pulses [Fig. 5(a)]. If the unchirped laser pulses are assumed to have a Gaussian shape with a FWHM of 229 fs, a linear chirp of  $1.30 \times 10^5 \text{ fs}^2$  is required to elongate the pulse duration to 283 fs. Using such incident chirped Gaussian pulses to perform the same simulation, we find pronounced disagreement between the simulated and observed spectra [Fig. 4(h)], even though the temporal shape of the incident Gaussian pulses approximates that of the incident soliton pulses [Fig. 5(a)]. All these simulation exercises have demonstrated the usefulness of the SPM-related spectral fringes in the rigorous quantification of the fiber continuum generation. Not surprisingly, at fiber output powers higher than the nonlinear polarization-mode depolarization onset (0.36 W, Fig. 3), significant deviation between the observed and simulated spectra is always found.

## 5. Discussions

### 5.1 Remarks on simulating fiber continuum generation by the GNLSE

The main result of this work (Fig. 4) demonstrates the feasibility of rigorous quantification of fiber continuum generation by the scalar GNLSE. Considering the relatively restrictive experimental conditions in use, we believe the lack of such rigorous quantification in the literature is mainly due to the poorly controlled experiments, rather than the oversimplifications in deriving the scalar GNLSE, such as the slowly varying envelope approximation. Although this work reports a rather specific fiber continuum generation, the methodology of the corresponding GNLSE simulation may be generalized to two broader cases. First, the current work may serve as a starting point to understand the nonlinear polarization-mode depolarization using the more advanced tools of the vector-based GNLSE. This will permit quantitative interpretation of unpolarized fiber continuum generation. Second, the same methodology may be applied to conventional supercontinuum generation by

various ZDW PCFs, which have produced the broadest bandwidth. If the incident pulses and the fiber dispersion are well-characterized, the influences of the frequency dependence of modal effective area [32] and the input noise [27] may be quantified independently.

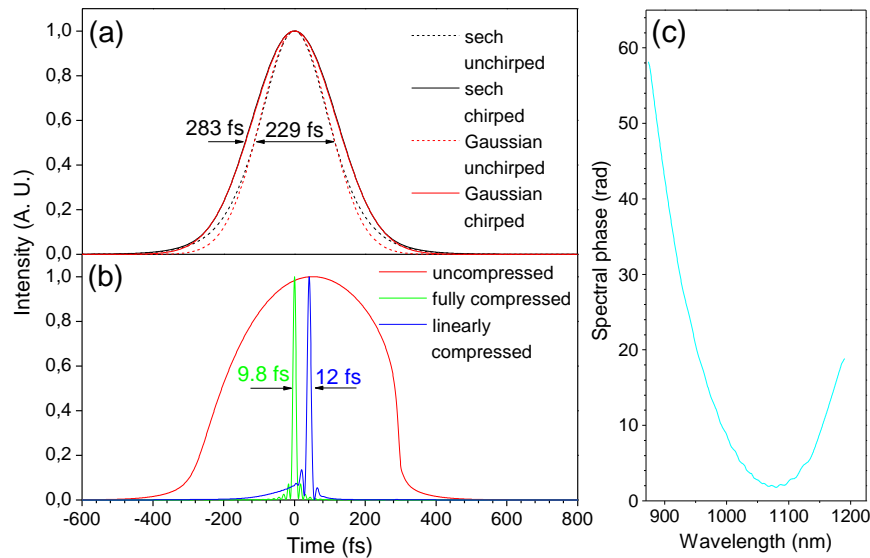


Fig. 5. (a) Temporal profiles of unchirped and chirped incident sech (or Gaussian) pulses with FWHM widths of 229 fs and 283 fs, respectively. (b) Temporal profiles of output continuum pulses at fiber output power of 0.361 W without compression, with compression removing linear chirp, and with compression removing full chirp. (c) Simulated spectral phase of the uncompressed continuum pulses at fiber output power of 0.361 W.

### 5.2 Pulse compression/shaping of fiber continua

Because the simulated spectrum at fiber output power of 0.361 W is in quantitative agreement with the observed spectrum [Fig. 4(d)], the correspondingly simulated temporal profile [Fig. 5(b)] and the spectral phase [Fig. 5(c)] of the continuum pulses are considered to be quantitatively correct. The temporal profile exhibits a self-steepening at the trailing edge of the pulses, which is likely responsible for the observed asymmetry of spectral broadening [Fig. 4(d)]. Nevertheless, no pulse splitting is observed in the time domain after the spectral broadening, suggesting that the continuum pulses are suitable for pulse compression. The spectral phase of the continuum pulses can be approximated by a linear positive chirp of  $680 \text{ fs}^2$ . The removal of this chirp by introducing a compensating linear negative chirp results in a compressed pulse width of 12 fs, approximating the related transform-limited (TL) value of 9.8 fs [Fig. 5(b)]. The pronounced pedestal and sidelobes cannot be prevented by fine tuning the compensating linear negative chirp, indicating the limitation of pulse compression by a prism pair (or grating pair). Consistently, previous attempts to compress similarly generated fiber continua by a grating or prism compressor were unable to compress the pulses close to the TL width [13,14]. More noticeably, the temporal profile of the compressed pulses free of linear chirp [Fig. 5(b)] unusually resembles that measured in Fig. 5 of Ref. 13. These observations reveal the usefulness of the rigorously quantified fiber continua in guiding the pulse compression. In order to compress the continuum pulses close to their TL widths, rigorous quantification asserts that it is necessary to simultaneously remove the linear and nonlinear chirp of the continuum pulses by a spatial light modular (SLM) (Table 1).

One particularly attractive pulse compression/shaping scheme is the combination of the rigorously quantified fiber continuum generation with the multiphoton intrapulse interference phase scan (MIIPS) method for simultaneous phase measurement and compensation of femtosecond laser pulses [33,34]. The rigorously quantified fiber continua allow the calibration of MIIPS-assisted pulse measurement, while the calibrated MIIPS-assisted pulse measurement permits arbitrary pulse measurement and shaping of other unknown pulses spectrally overlapping with the fiber continua. Another attractive pulse compression scheme is the combination of an all-fiber Yb laser-based femtosecond source [35,36] with a SLM-type pulse compressor. The envelope of the femtosecond pulses from the Yb fiber laser, once measured by methods such as cross-correlation frequency-resolved optical grating (X-FROG) or spectral phase interferometry for direct electric-field reconstruction (SPIDER), may produce similarly scalar GNLSE-quantified fiber continua amendable for the flexible pulse compression afforded by the SLM. Thus, the continuum-generating fiber may be spliced directly on the output fiber of the fiber laser [37] for maximum simplicity.

### 5.3 Routes toward alternative broadband coherent optical sources

One disadvantage of the PCF used in this study is that the bandwidth of the scalar GNLSE-quantified fiber continua is limited to  $\sim 300$  nm [Fig. 4(d)]. It is tempting to increase this bandwidth by selecting a longer fiber length. However, this effort has been unsuccessful due to the earlier onset of the nonlinear polarization-mode depolarization in a longer PCF. The experiment of Fig. 3 suggests that a larger unintentional linear birefringence is rather efficient to suppress the nonlinear polarization-mode depolarization. Thus, a polarization-maintaining DFDD-ANDiF with large ( $> 2 \times 10^{-5}$ ) built-in linear birefringence could be the ideal candidate for the PCF-based alternative broadband coherent optical sources (Fig. 1), providing the fiber is pumped along one principal axis of the fiber, and preferably, the slow axis. If the simple PCF design of Fig. 1 is used as the starting point, the powerful dispersion-engineering capability of PCFs along with certain intelligent designs may introduce the polarization-maintaining ability through symmetry-broken fiber guiding region, and at the same time, further decrease its normal dispersion, improve the flatness of the dispersion over a wider bandwidth, and increase the nonlinearity of the PCF. In contrast to the well-known dispersion-engineering of ZDW PCFs intended for generating the broadest supercontinuum, this polarization-maintaining DFDD-ANDiF represents another useful dispersion-engineered class of PCFs suitable for coherent continuum generation, leading to alternative broadband coherent optical sources with scalar GNLSE-quantified spectral-temporal properties. It should be noted that the continuum generation from the polarization-maintaining DFDD-ANDiF does not necessarily produce the fringed spectra of Fig. 4. Flat-top smooth continuum generation with broader bandwidths can be achieved if shorter incident laser pulses or longer fiber lengths are used [16]. In this case, however, the fringed continuum generation at a short fiber length (Fig. 4) may still be useful to validate the scalar GNLSE-based quantification, which would be difficult for the featureless smooth continuum generation.

While the above route intentionally introduces a large linear birefringence to suppress the weak unintentional intrinsic birefringence of the PCF (and the corresponding nonlinear polarization-mode depolarization), an alternative (and seemingly opposite) route is to completely avoid the weak unintentional birefringence by choosing fibers with perfect symmetry and with rotation symmetry of order higher than 2 [19], such as circular symmetry [15] and hexagonal symmetry [16]. The fibers of these symmetries are guaranteed to be non-birefringent [19], so that the fibers pumped by linearly polarized pulses can be effectively treated as polarization-maintaining fibers where the scalar GNLSE is valid [15,16]. This alternative route, although theoretically plausible, could be practically difficult. First, it is challenging to fabricate fibers with low ( $< 10^{-8}$ ) birefringence, so that the effect of nonlinear polarization-mode depolarization could be persistent. Second, the incident pulses could be slightly elliptical to excite the two degenerate polarization modes of a strictly non-birefringent fiber, so that the fiber output could be depolarized by cross-phase modulation [28].

## 6. Conclusions

A highly polarized fiber continuum source that can be rigorously quantified by the scalar GNLSE has been constructed using commercially available components. Due to the relatively high spectral density (1 mW/nm), long fiber length (90 mm), long pump pulse width (229 fs FWHM), and most importantly, the fully characterized pulse envelope, this source could be useful in applications where broadband ultrashort (<15 fs) pulse compression/shaping is required. Nonlinear polarization-mode depolarization is identified as the key factor that limits the bandwidth of the current source. Improved polarization-maintained fiber design should overcome this limiting factor to result in a series of attractive alternative broadband coherent optical sources based on birefringent DFDD-ANDiF. The corresponding scalar GNLSE-quantified fiber continua can guide the pulse compression procedure necessary for ultra-broadband coherent control in ultrafast spectroscopy and microscopy.

## Acknowledgments

This work was supported in part by grants from the National Institutes of Health (NIH) (NCI R33 CA115536; NIBIB R01 EB009073; NCI RC1 CA147096, S.A.B.). Additional information can be found at <http://biophotonics.illinois.edu>.